Theoretical Analysis of the Second-order Synchrosqueezing Transform

Ratikanta Behera, Sylvain Meignen, Thomas Oberlin

Theoretical Analysis of the Second-order Synchrosqueezing Transform

Ratikanta Behera[1], Sylvain Meignen[2], and Thomas Oberlin[3]
[1,2]Jean Kuntzmann laboratory,
Joseph Fourier University,
51 rue des mathematiques,
38041 Grenoble cedex 09,France.
[3] INP - ENSEEIHT Toulouse,
2 rue Charles Camichel, B.P. 7122,
31071 Toulouse Cedex 7, FRANCE.

Abstract

We consider in this article the analysis of multicomponent signals, defined as superpositions of modulated waves also called modes. More precisely, we focus on the analysis of a variant of the second-order synchrosqueezing transform, which was introduced recently, to deal with modes containing strong frequency modulation. Before going into this analysis, we revisit the case where the modes are assumed to be with weak frequency modulation as in the seminal paper of Daubechies et *al.* [8], to show that the constraint on the compactness of the analysis window in the Fourier domain can be alleviated. We also explain why the hypotheses made on the modes making up the multicomponent signal must be different when one considers either wavelet or short–time Fourier transform–based synchrosqueezing. The rest of the paper is devoted to the theoretical analysis of the variant of the second order synchrosqueezing transform [16] and numerical simulations illustrate the performance of the latter.

Keywords: time-frequency analysis; synchrosqueezing transform; multicomponent signals.

[1]Email:ratikanta.maths@gmail.com
[2]Email:sylvain.meignen@imag.fr
[3]Email:thomas.oberlin@enseeiht.fr

1. Introduction

Multicomponent signals (MCs) are encountered in a number of fields of practical interest such as meteorology, structural stability analysis, and medical studies - see, e.g., [6, 7, 11, 12]. Linear time-frequency (TF) analysis techniques have been extensively used to analyze and process these signals [14], the method to be used depending on the nature of the modes making up the signal. Standard linear TF methods such as the short-time Fourier transform (STFT) and the continuous wavelet transform (CWT) are commonly used to analyze such signals. In that context, the reassignment method (RM) was developed [1] to improve the readability of these linear TF representations. Unfortunately, since RM applies to the magnitude of the studied TF transform, the method results in a loss of information and the reassigned representation is not sufficient to recover the original signal.

Recently, Daubechies et *al.* [8] showed interesting results on the so-called synchrosqueezing transform (SST) to represent MCs, a method introduced in the mid-1990s for audio signal analysis [9]. SST combines the localization and sparsity properties of RM with the invertibility of a traditional TF representation. Originally proposed as a post-processing method applied to the CWT, SST can alternatively be applied to STFT with minor changes [15], to obtain the so-called FSST. Since the seminal paper of Daubechies et al. [8], many new developments have been carried out in various directions. First, an extension to the bidimensional case was proposed in [5], while a generalization of the wavelet approach by means of wavelet packets decomposition for both one dimensional and bidimensional cases is available in [26, 25]. Finally, it is also worth noting that a study of synchrosqueezing applied to a more general class of multicomponent signals was done in [22].

In the present paper, we focus on what essentially limits the applicability of SST which are, on the one hand, the hypotheses of weak frequency modulation for the modes making up the signal and, on the other hand, the compactness of the frequency support of the analysis window. To better take into account the frequency modulation, in the FSST context, a first approach based on the definition of a demodulation operator was proposed in [13], while a new synchrosqueezing operator based on a new chirp rate estimate was defined in [16, 2]. However, in these last two papers, no theoretical

analysis of the proposed new synchrosqueezing transform was provided. To deal with this issue is the main aim of this paper.

While pursuing this goal, we will pay particular attention to use non compactly supported window in the frequency domain. Indeed, the main problem induced by using windows compactly supported in the frequency domain is that they are not adapted to deal with real-time computations. To deal with this issue, a new wavelet-based SST defined using wavelet with sufficiently many vanishing moments and a minimum support in the time domain was proposed in [4], but the mathematical study of the corresponding instantaneous frequency (IF) estimates is still under development. In the meantime, an extension of synchrosqueezing based on wavelet packets not compactly supported in the frequency domain along with its mathematical analysis was developed in [24]. In the context of this paper, the focus is put on the Fourier-based SST, when the analysis window is not compactly supported. We first revisit the case of weak modulation for the modes using such a type of window, and then prove a new approximation theorem on a slightly different version of the synchrosqueezing transform proposed in [16].

The outline of the paper is as follows: in Section 2, we recall some notation and definitions. In Section 3, we introduce FSST and wavelet-based SST (WSST) along with the corresponding approximation results and explain why the hypotheses on the phase of the modes have to be different. Then, after having introduced some necessary ingredients, we derive, in Section 4, the approximation theorem for the second order synchrosqueezing transform, showing that this new transform is fully adapted for analyzing modes with strong frequency modulations. Finally, numerical illustrations conclude the paper.

2. Definitions

2.1. Short-time Fourier transform

We denote by $L^1(\mathbb{R})$ and $L^2(\mathbb{R})$ the space of integrable, and square integrable functions. Consider a signal $f \in L^1(\mathbb{R})$, and take a window g in the Schwartz class, $\mathcal{S}(\mathbb{R})$, the space of smooth functions with fast decaying derivatives of any order; its Fourier transform is defined by:

$$\widehat{f}(\eta) = \mathcal{F}\{f\}(\eta) = \int_{\mathbb{R}} f(\tau) e^{-2i\pi\eta\tau} d\tau. \tag{1}$$

The need for time-localized frequency descriptors leads to short-time Fourier transform (STFT) which is obtained through the use of a sliding window $g \in L^2(\mathbb{R})$ defined by:

$$V_f^g(\eta, t) = \int_{\mathbb{R}} f(\tau) g(\tau - t) e^{-2i\pi\eta(\tau - t)} d\tau \tag{2}$$

$$= \int_{\mathbb{R}} f(t + \tau) g(\tau) e^{-2i\pi\eta\tau} d\tau \quad = \mathbb{A}(\eta, t) e^{2i\pi\Phi(\eta,t)}. \tag{3}$$

The representation of $|V_f^g(\eta, t)|^2$ in the TF plane is called the spectrogram of f. The STFT admits the following synthesis formula (provided the window g does not vanish and is continuous at 0):

$$f(t) = \frac{1}{g(0)^*} \int_{\mathbb{R}} V_f^g(\eta, t) d\eta. \tag{4}$$

Further, if the signal is analytic (i.e. $\eta \leq 0 \Rightarrow \hat{f}(\eta) = 0$) then the integral domain for η is restricted to $\mathbb{R}_+$.

2.2. Continuous wavelet transform

Let us consider an admissible wavelet $\psi \in L^2(\mathbb{R})$, satisfying $0 < C_\psi = \int_0^\infty |\widehat{\psi}(\xi)|^2 \frac{d\xi}{\xi} < \infty$ and then define for any time t and scale $a > 0$, the *continuous wavelet transform* (CWT) of f by:

$$W_f^\psi(a, t) = \frac{1}{a} \int_{\mathbb{R}} f(\tau) \psi \left(\frac{\tau - t}{a} \right)^* d\tau, \tag{5}$$

where z^* denotes the complex conjugate of z. Assuming that ψ is analytic, i.e. $\mathrm{Supp}(\widehat{\psi}) \subset [0, \infty[$, and f real-valued, the CWT admits the following synthesis formula (Morlet formula):

$$f(t) = 2\mathcal{R} \left\{ \frac{1}{C'_\psi} \int_0^\infty W_f^\psi(a, t) \frac{da}{a} \right\}, \tag{6}$$

where $\mathcal{R}$ denotes the real part of a complex number and $C'_\psi = \int_0^\infty \widehat{\psi}^*(\xi) \frac{d\xi}{\xi}$.

2.3. Multicomponent signal

In the present paper, we analyze so-called *multicomponent signals* of the form,

$$f(t) = \sum_{k=1}^{K} f_k(t), \quad \text{with } f_k(t) = A_k(t) e^{2i\pi\phi_k(t)}, \tag{7}$$

for some K, where $A_k(t)$ and $\phi_k(t)$ are time-varying amplitude and phase functions respectively such that $A_k(t) > 0$, $\phi_k'(t) > 0$ and $\phi_{k+1}'(t) > \phi_k'(t)$ for all t. In the following, $\phi_k'(t)$ is often called instantaneous frequency (IF) of mode k and $A_k(t)$ its instantaneous amplitude (IA). One of the goal of TF analysis is to recover the instantaneous frequencies $\{\phi_k'(t)\}_{1\leq k\leq K}$ and amplitudes $\{A_k(t)\}_{1\leq k\leq K}$, from a given TF representation of f. Note that, if we are given real-valued functions, i.e. $f_k(t) = A_k(t)\cos(2\pi\phi_k(t))$, we can still derive the same analysis by considering analytic windows or wavelets, as soon as $\phi_1'(t) > \Delta\, \forall t$.

3. Synchrosqueezing transform

The synchrosqueezing transform (SST) is an approach originally introduced in the context of audio signals [9], whose theoretical analysis was recently carried out in [8]. It belongs to the family of TF reassignment methods and corresponds to a nonlinear operator that sharpens the TF representation of a signal while enabling mode reconstruction. Moreover, SST combines the localization and sparsity properties of TF reassignment with the invertibility property of traditional TF transforms, and is robust to a variety of signal perturbations [18]. The key ingredient to SST is an IF estimate computed from the TF representation, which we introduce now. The results enounced in the next two subsections are not new, but we recall them for the sake of consistency and also because they ease the understanding of the following parts of the paper. They were originally stated in [8] in the wavelet case, and in [15][21] for that of STFT.

3.1. Computation of IF estimate in the TF plane

In the STFT framework, the IF of signal f at time t and frequency η can be estimated, wherever $V_f^g(\eta,t) \neq 0$, by [1]:

$$\begin{aligned} \widehat{\omega}_f(\eta,t) &:= \frac{1}{2\pi}\partial_t arg V_f^g(\eta,t), \\ &= \partial_t \Phi(\eta,t) \text{ defined in (2)}, \\ &= \mathcal{R}\left(\frac{1}{2i\pi}\frac{\partial_t V_f^g(\eta,t)}{V_f^g(\eta,t)}\right). \end{aligned} \tag{8}$$

Note that the quantity of which we take the real part:

$$\tilde{\omega}_f(\eta,t) = \frac{\partial_t V_f^g(\eta,t)}{2i\pi V_f^g(\eta,t)}, \tag{9}$$

is useful to more theoretical investigations but should not be used to estimate real quantities such as IF. Similar quantities can be derived in the CWT case as follows: $\widehat{\omega}_f(a,t) = \mathcal{R}\left(\widetilde{\omega}_f(a,t)\right)$, with $\tilde{\omega}_f(a,t) = \frac{1}{2i\pi}\frac{\partial_t W_f^\psi(a,t)}{W_f^\psi(a,t)}$.

Remark 1. In [8], the estimate $\widetilde{\omega}_f(a,t)$ is used instead of $\widehat{\omega}_f(a,t)$. However, most theorems are valid only for a real estimate as will be shown later.

3.2. STFT-based synchrosqueezing transform

Definition 1. *Let $\varepsilon > 0$ and $\Delta > 0$. The set $\mathcal{B}_{\Delta,\varepsilon}$ of multicomponent signals with modulation ε and separation Δ is the set of all multicomponent signals defined in* (7) *satisfying:*

$$\begin{aligned} &A_k \in C^1(\mathbb{R}) \cap L^\infty(\mathbb{R}), \phi_k \in C^2(\mathbb{R}), \\ &\sup_{t\in\mathbb{R}} \phi_k'(t) < \infty, \phi_k'(t) > 0, A_k(t) > 0, \quad \forall t \\ &|A_k'(t)| \leq \varepsilon, |\phi_k''(t)| \leq \varepsilon \quad \forall t \in \mathbb{R}. \end{aligned} \tag{10}$$

Further, the f_ks are separated with resolution Δ, i.e., for all $k \in \{1,...,K-1\}$ and all t,

$$\phi_{k+1}'(t) - \phi_k'(t) \geq 2\Delta. \tag{11}$$

Definition 2. *Let h be a L^1-normalized positive function belonging to $C_c^\infty(\mathbb{R})$, the space of compactly supported smooth function, and pick $\gamma, \lambda > 0$. The STFT-based synchrosqueezing (FSST) of f with threshold γ and accuracy λ is defined by:*

$$T_f^{\lambda,\gamma}(\omega,t) = \frac{1}{g(0)} \int_{|V_f^g(\eta,t)|>\gamma} V_f^g(\eta,t) \frac{1}{\lambda} h\left(\frac{\omega - \widehat{\omega}_f(\eta,t)}{\lambda}\right) d\eta. \tag{12}$$

If we make λ and γ tend to zero, then $T_f^{\lambda,\gamma}(\omega,t)$ tends to some value which we formally write as:

$$T_f(\omega,t) = \frac{1}{g(0)} \int_{\mathbb{R}} V_f^g(\eta,t) \delta(\omega - \widehat{\omega}_f(\eta,t)) d\eta, \tag{13}$$

called FSST in the sequel, and where δ is the Dirac distribution.

Theorem 1. *Consider $f \in \mathcal{B}_{\Delta,\varepsilon}$ and put $\tilde{\varepsilon} = \varepsilon^{1/3}$. Let $g \in \mathcal{S}(\mathbb{R})$, the Schwartz class, be such that supp$(\widehat{g}) \subset [-\Delta, \Delta]$. Then, if ε is small enough, the following holds:*

(a) $|V_f^g(\eta,t)| > \tilde{\varepsilon}$ only when there exists $k \in \{1,...,K\}$ such that $(\eta,t) \in Z_k := \{(\eta,t),\ s.t.\ |\eta - \phi_k'(t)| < \Delta\}$.

(b) For all $k \in \{1,...,K\}$ and all $(\eta,t) \in Z_k$ such that $|V_f^g(\eta,t)| > \tilde{\varepsilon}$, we have

$$|\widehat{\omega}_f(\eta,t) - \phi_k'(t)| \leq \tilde{\varepsilon}. \tag{14}$$

(c) For all $k \in \{1,...,K\}$, there exists a constant C such that for all $t \in \mathbb{R}$,

$$\left| \lim_{\lambda \to 0} \left(\int_{|\omega - \phi_k'(t)| < \tilde{\varepsilon}} T_f^{\lambda,\tilde{\varepsilon}}(\omega,t) dw \right) - f_k(t) \right| \leq C\tilde{\varepsilon}. \tag{15}$$

Proof. This theorem gives a strong approximation result for the class $\mathcal{B}_{\Delta,\varepsilon}$, since it ensures that the non-zero coefficients of the FSST are localized around the curves $(t, \phi_k'(t))$, and that the reconstruction of the modes is easily obtained from the concentrated representation. The main steps of the proof are detailed hereafter.

(a) For any $(\eta, t) \in \mathbb{R}^2$, a zeroth order Taylor expansion of the amplitude and first order expansion of the phase of the modes lead to:

$$|V_f^g(\eta, t) - \sum_{k=1}^{K} f_k(t)\hat{g}(\eta - \phi_k'(t))| \leq \varepsilon\Gamma_1(t), \tag{16}$$

where $\Gamma_1(t) = KI_1 + \pi I_2 \sum_{k=1}^{K} A_k(t)$, and $I_n = \int_{\mathbb{R}} |x|^n |g(x)| dx$. If

$$\tilde{\varepsilon} \leq \|\Gamma_1\|_\infty^{-\frac{1}{2}}, \tag{17}$$

and since $\hat{g}$ is compactly supported in $[-\Delta, \Delta]$, and the IFs of the modes are separated by more than 2Δ, we have, for any $(\eta, t) \notin \bigcup_{k=1}^{K} Z_k$:

$$|V_f^g(\eta, t)| \leq \varepsilon\Gamma_1(t) \leq \tilde{\varepsilon}. \tag{18}$$

(b) Now, we derive the same kind of estimate for $\partial_t V_f^g$. Since $V_f^g(\eta, t)$ is differentiable with respect to both variables, and that for any $(\eta, t) \in \mathbb{R}^2$:

$$\partial_t V_f^g(\eta, t) = 2i\pi\eta V_f^g(\eta, t) - V_f^{g'}(\eta, t). \tag{19}$$

The counterpart of equation (16) is then:

$$|\partial_t V_f^g(\eta, t) - 2i\pi \sum_{k=1}^{K} f_k(t)\phi_k'(t)\hat{g}(\eta - \phi_k'(t))| \leq \varepsilon \left(\Gamma_2(t) + 2\pi|\eta|\Gamma_1(t)\right), \tag{20}$$

where $\Gamma_2(t) = KI_1' + \pi I_2' \sum_{k=1}^{K} A_k(t)$, with $I_n' = \int_{\mathbb{R}} |t|^n |g'(t)| dt$.

Now, we can remark that, since the sets Z_k are disjoint, there is at most one non-zero term in the sums involved in equations (16) and (20). We can thus write for any $(\eta, t) \in Z_k$:

$$\begin{aligned}
&|\hat{\omega}_f(\eta, f) - \phi_k'(t)| \\
&\leq \left| \frac{\partial_t V_f^g(\eta, t) - 2i\pi\phi_k'(t) f_k(t)\hat{g}(\eta - \phi_k'(t))}{2i\pi V_f^g(\eta, t)} \right| + \left| \frac{\phi_k'(t)(f_k(t)\hat{g}(\eta - \phi_k'(t)) - V_f^g(\eta, t))}{V_f^g(\eta, t)} \right| \\
&\leq \frac{\varepsilon\left(\Gamma_2(t) + 2\pi|\eta|\Gamma_1(t)\right)}{2\pi\tilde{\varepsilon}} + \phi_k'(t)\frac{\varepsilon\Gamma_1(t)}{\tilde{\varepsilon}} \\
&\leq \tilde{\varepsilon}^2 \left(\frac{\Gamma_2(t)}{2\pi} + (|\eta| + \phi_k'(t))\Gamma_1(t) \right).
\end{aligned}$$

Hence, if ε is sufficiently small, i.e. if it satisfies for all t

$$\tilde{\varepsilon} \leq \left(\frac{\Gamma_2(t)}{2\pi} + (2\phi_k'(t) + \Delta)\Gamma_1(t) \right)^{-1}, \tag{21}$$

one obtains

$$|\hat{\omega}_f(\eta, t) - \phi_k'(t)| \leq \tilde{\varepsilon}. \tag{22}$$

Remark 2. Note that the proof of points (a) and (b) are also available in [19], but with different hypotheses. Indeed, in that paper, the constraints on the modes are non-local, i.e. $\|A_k'\|_\infty \leq \varepsilon \|\phi_k'\|_\infty$ and $\|\phi_k''\|_\infty \leq \varepsilon \|\phi_k'\|_\infty$ (Definition 3.1 in [19]). As we shall see later on, when analyzing the behavior of $\hat{\omega}_f(\eta, t)$ on a linear chirp, the quality of the estimate is only related to the amplitude of ϕ'', which will justify the hypothesis we put on ϕ''. A more important difference with [19] involves the separation condition satisfied by the different modes making up the signal (Definition 3.2 in [19]):

$$\inf_t \phi_k'(t) - \sup_t \phi_{k-1}'(t) > 2\Delta, \tag{23}$$

which is much stronger than condition (11). For instance, the simple signals whose STFT are depicted in Figure 1 (first column) do not satisfy hypothesis (23).

(c) Let $t \in \mathbb{R}$, using the same type of technique as in [8] (Estimate 3.9), one can write:

$$\lim_{\lambda \to 0} \int_{|\omega - \phi_k'(t)| < \tilde{\varepsilon}} T_f^{\lambda, \tilde{\varepsilon}}(\omega, t)\, d\omega \;\; = \frac{1}{g(0)^*} \int_{\{|V_f^g(\eta,t)| > \tilde{\varepsilon}\} \bigcap \{|\hat{\omega}(\eta,t) - \phi_k'(t)| < \tilde{\varepsilon}\}} V_f^g(\eta, t)\, d\eta.$$

We now prove that the integration interval of the last equation, denoted by $X = \{|V_f^g(\eta, t)| > \tilde{\varepsilon}\} \bigcap \{|\hat{\omega}_f(\eta, t) - \phi_k'(t)| < \tilde{\varepsilon}\}$, equals the following set:

$$Y = \{|V_f^g(\eta, t)| > \tilde{\varepsilon}\} \bigcap \{|\eta - \phi_k'(t)| < \Delta\}.$$

If $\eta \in X$, it is such that $|V_f^g(\eta, t)| > \tilde{\varepsilon}$ and $|\hat{\omega}_f(\eta, t) - \phi_k'(t)| < \tilde{\varepsilon}$. Also, from (a) there exists a unique l such that $(\eta, t) \in Z_l$. If $l \neq k$, we would have:

$$\begin{aligned} |\hat{\omega}_f(\eta, t) - \phi_k'(t)| &\geq |\phi_l'(t) - \phi_k'(t)| - |\hat{\omega}_f(\eta, t) - \phi_l'(t)| \\ &\geq 2\Delta - \tilde{\varepsilon}, \end{aligned}$$

because of (b). Taking $\tilde{\varepsilon} \leq \Delta$, we get $|\hat{\omega}_f(\eta, t) - \phi_k'(t)| \geq \tilde{\varepsilon}$, which contradicts $\eta \in X$. Hence, $l = k$ and $X \subset Y$. Conversely, if $\eta \in Y$, equation (26) immediately shows $\eta \in Y$, hence $X = Y$.

Finally,

$$
\begin{aligned}
&\left| \lim_{\lambda \to 0} \left(\int_{|\omega - \phi_k'(t)| < \tilde{\varepsilon}} T_f^{\lambda, \tilde{\varepsilon}}(\omega, t)\, d\omega \right) - f_k(t) \right| \\
&= \left| \frac{1}{g(0)^*} \int_{\{|V_f^g(\eta,t)| > \tilde{\varepsilon}\} \bigcap \{|\eta - \phi_k'(t)| < \Delta\}} V_f^g(\eta, t)\, d\eta - f_k(t) \right| \\
&= \left| \frac{1}{g(0)^*} \int_{\{|\eta - \phi_k'(t)| < \Delta\}} V_f^g(\eta, t)\, d\eta - f_k(t) - \frac{1}{g(0)^*} \int_{\{|\eta - \phi_k'(t)| < \Delta\} \bigcap \{|V_f^g(\eta,t)| \leq \tilde{\varepsilon}\}} V_f^g(\eta, t)\, d\eta \right| \\
&\leq \left| \frac{1}{g(0)^*} \int_{\{|\eta - \phi_k'(t)| < \Delta\}} V_f^g(\eta, t)\, d\eta - f_k(t) \right| + \frac{2\Delta}{|g(0)|} \tilde{\varepsilon} \\
&\leq \left| \frac{1}{g(0)} \int_{\{|\eta - \phi_k'(t)| < \Delta\}} f_k(t) \hat{g}(\eta - \phi_k'(t))\, d\eta - f_k(t) \right| \\
&\qquad + \frac{1}{|g(0)|} \int_{\{|\eta - \phi_k'(t)| < \Delta\}} \left| V_f^g(\eta, t) - f_k(t) \hat{g}(\eta - \phi_k'(t)) \right| d\eta + \frac{2\Delta}{|g(0)|} \tilde{\varepsilon} \\
&\leq 0 + \frac{2\Delta}{|g(0)|} \varepsilon \Gamma_1(t) + \frac{2\Delta}{|g(0)|} \tilde{\varepsilon} \\
&\leq \frac{4\Delta}{|g(0)|} \tilde{\varepsilon}.
\end{aligned}
$$

□

3.3. Generalization to non-compactly supported $\hat{g}$

In the above section, we assumed that $\hat{g}$ was compactly supported. We here explain that we can state the same approximation result while relaxing this strong condition.

Theorem 2. *Assume that there exist constants M_1, $M_2 > 0$ such that $g \in \mathcal{S}(\mathbb{R})$ satisfies:*

$$
\begin{aligned}
&\textit{For all } |\eta| > \Delta,\ |\hat{g}(\eta)| \leq M_1 \varepsilon, \\
&\textit{and } \int_{|\eta| > \Delta} |\hat{g}(\eta)|\, d\eta \leq M_2 \tilde{\varepsilon}.
\end{aligned}
$$

Then all conclusions of Theorem 1 remain valid.

Proof. (a) We first remark that equation (16) remains valid for any (η, t):

$$|V_f^g(\eta,t) - \sum_{k=1}^{K} f_k(t)\widehat{g}(\eta - \phi_k'(t))| \leq \varepsilon\Gamma_1(t).$$

If we assume that for any t,

$$\tilde{\varepsilon} \leq \min\left[\frac{1}{2}\left(M_1\sum_{k=1}^{K}A_k(t)\right)^{-1}, \frac{1}{2}\Gamma_1(t)^{-\frac{1}{2}}\right], \tag{24}$$

then we get, for any $(\eta,t) \notin \bigcup_{k=1}^{K} Z_k$:

$$|V_f^g(\eta,t)| \;\leq\; \varepsilon\left(M_1\sum_{k=1}^{K}A_k(t) + \Gamma_1(t)\right) \leq \tilde{\varepsilon}.$$

If $(\eta,t) \in Z_k$, $|V_f^g(\eta,t) - f_k(t)\widehat{g}(\eta-\phi_k'(t))| \leq \varepsilon\left(M_1\sum_{l\neq k}A_l(t) + \Gamma_1(t)\right) \leq \tilde{\varepsilon}^2$.

(b) Similarly, we still have estimate (20) for any (η,t). If we assume that for all $k \in \{1,\cdots,K\}$ and for all t,

$$\tilde{\varepsilon} \leq \min\left[\frac{1}{2}\left(M_1\sum_{l\neq k}\phi_l'(t)A_l(t)\right)^{-1}, \frac{1}{2}\left(\frac{\Gamma_2(t)}{2\pi} + (2\phi_k'(t)+\Delta)\Gamma_1(t)\right)^{-1}\right], \tag{25}$$

then we get for any $(\eta,t) \in Z_k$ such that $|V_f^g(\eta,t)| \geq \tilde{\varepsilon}$:

$$|\hat{\omega}_f(\eta,f) - \phi_k'(t)| \leq \tilde{\varepsilon}. \tag{26}$$

(c) Regarding point (c) of Theorem 1, the only difference when one considers a non compactly supported window appears at the very end of the proof. More precisely, the following term is not zero anymore, but can be bounded in the following way:

$$\begin{aligned}\left|\frac{1}{g(0)}\int_{|\eta-\phi_k'(t)|<\Delta} f_k(t)\hat{g}(\eta-\phi_k'(t))\,d\eta - f_k(t)\right| &\leq \frac{A_k(t)}{|g(0)|}\int_{|\eta|>\Delta}|\hat{g}(\eta)|\,d\eta \\ &\leq \frac{A_k(t)M_2}{|g(0)|}\tilde{\varepsilon}.\end{aligned}$$

Thus, point (c) of the theorem still holds, but with constant

$$C = \frac{4\Delta + \max_k \|A_k\|_\infty M_2}{|g(0)|}.$$

□

Remark 3. Let us remark that this extended result requires stronger assumptions on $\tilde{\varepsilon}$: conditions (17) and (21) are replaced by (24) and (25), respectively.

Remark 4. It is interesting to remark also that $f_k(t)\hat{g}(\eta - \phi_k'(t)) = V_{f_k^1}^g(\eta, t)$ with $f_k^1(\tau) = A_k(t)e^{2i\pi(\phi_k(t)+(\tau-t)\phi_k'(t))}$. Then, the right hand side of equations (16) and (20) can be rewritten respectively as $|V_f^g(\eta,t) - V_{f_k^1}^g(\eta,t)|$ and $|\partial_t V_f^g(\eta,t) - \partial_t V_{f_k^1}^g(\eta,t)|$ so that Theorem 1 is based on the STFT of a constant amplitude and first order phase approximation of the kth mode.

3.4. Wavelet based synchrosqueezing transform [8]

We now recall the definition of SST in the wavelet framework.

Definition 3. *Let $\varepsilon > 0$ and $\Delta \in (0,1)$. The set $\mathcal{A}_{\Delta,\varepsilon}$ of multicomponent signals with modulation ε and separation Δ corresponds to signals defined in (7) with f_k satisfying:*

$$\begin{aligned} &A_k \in C^1(\mathbb{R}) \cap L^\infty(\mathbb{R}), \phi_k \in C^2(\mathbb{R}), \\ &\inf_{t\in\mathbb{R}} \phi_k'(t) > 0, \sup_{t\in\mathbb{R}} \phi_k'(t) < \infty, A_k(t) > 0, \\ &|A_k'(t)| \le \varepsilon\phi_k'(t), |\phi_k''(t)| \le \varepsilon\phi_k'(t) \quad \forall t \in \mathbb{R}. \end{aligned} \tag{27}$$

Further, the f_ks are separated with resolution Δ, i.e., for all $k \in \{1, \cdots, K-1\}$ and all t

$$|\phi_{k+1}'(t) - \phi_k'(t)| \ge \Delta(\phi_{k+1}'(t) + \phi_k'(t)). \tag{28}$$

Definition 4. *Let h be a positive L^1-normalized window belonging to $C_c^\infty(\mathbb{R})$, and consider $\gamma, \lambda > 0$, the wavelet-based synchrosqueezing (WSST) of f with threshold γ and accuracy λ is defined by:*

$$S_f^{\lambda,\gamma}(\omega,t) := C_\psi'^{-1} \int_{|W_f^\psi(a,t)|>\gamma} W_f^\psi(a,t) \frac{1}{\lambda} h\left(\frac{\omega - \hat{\omega}_f(a,t)}{\lambda}\right) \frac{da}{a}. \tag{29}$$

Theorem 3. *Let $f \in \mathcal{A}_{\Delta,\varepsilon}$, and set $\tilde{\varepsilon} = \varepsilon^{\frac{1}{3}}$. Let ψ be a wavelet belonging to $\mathcal{S}(\mathbb{R})$ such that $\widehat{\psi}$ is supported in $[1-\triangle, 1+\triangle]$. Then, provided ε is sufficiently small, the following hold:*

(a) $|W_f^{\psi}(a,t)| \geq \tilde{\varepsilon}$ only when, there exists $k \in \{1, ..., K\}$, such that for each pair $(a,t) \in Z_k := \{(a,t),\ s.t.\ |a\phi_k'(t) - 1| < \Delta\}$.

(b) For each $k \in \{1, ..., K\}$ and then for all $(a,t) \in Z_k$ for which holds $|W_f^{\psi}(a,t)| > \tilde{\varepsilon}$, we have

$$|\widehat{\omega}_f(a,t) - \phi_k'(t)| \leq \tilde{\varepsilon}. \tag{30}$$

(c) Moreover, for each $k \in \{1, ..., K\}$, there exists a constant C such that for any $t \in \mathbb{R}$

$$\left| \lim_{\lambda \to 0} \int_{|\omega - \phi_k'(t)| < \tilde{\varepsilon}} S_f^{\lambda,\tilde{\varepsilon}}(\omega, t) d\omega - f_k(t) \right| \leq C\tilde{\varepsilon}. \tag{31}$$

Proof. This theorem is proved in [8] and gives a strong approximation result for the class $\mathcal{A}_{\Delta,\varepsilon}$, since it ensures that the non-zero coefficients of the WSST are localized around the curves $(t, \frac{1}{\phi_k'(t)})$ in the time-scale space, and that the reconstruction of the modes is easily obtained from the concentrated representation. □

Remark 5. It is worth mentioning here that to consider compactly supported WSSTs in the frequency domain is crucial to ensure accurate estimations. However, these TF representations are not compatible with real-time applications, therefore new approaches have been proposed in that direction. For instance, in [4], wavelets are designed with sufficiently many vanishing moments and a minimum support in the time domain, the mathematical analysis of such a new model being still under development.

Remark 6. Pure waves obviously satisfy the assumptions of Theorems 1 and 3 for any ε. However, for modulated waves the assumptions for FSST and WSST are different because, in the FSST context, the assumption on the frequency modulation $\phi''(t)$ does not depend on the IF. This is due to the fact that in the STFT framework, the frequency resolution does not depend on the frequency, whereas in the wavelet case it depends on the scale.

To make this clearer in the STFT context, we consider the IF estimate computed on a linear chirp, i.e., a wave with linear instantaneous frequency. To carry out this study, we compute STFT with a Gaussian window $g(t) = e^{-\pi t^2}$. To choose such a window is interesting for our purpose, because one has a closed form expression for the STFT of a linear chirp, as recalled hereafter.

The study of the IF estimate $\hat{\omega}_f(\eta, t)$ for a linear chirp requires the following lemma:

Lemma 1. *Consider $u(t) = e^{-\pi z t^2}$, where $z = re^{i\theta}$ with $\cos\theta > 0$, so that u is integrable. Then its Fourier transform reads*

$$\hat{u}(\xi) = r^{\frac{-1}{2}} e^{-i\frac{\theta}{2}} e^{-\frac{-\pi}{re^{i\theta}}\xi^2}. \tag{32}$$

Proof. This result is straightforward as one can proceed as in the case z real. □

Then, consider the linear chirp $h_c(\tau) = Ae^{2i\pi\phi(\tau)}$, where ϕ is a quadratic polynomial. To start with, we remark that $h_c(\tau)$ can be written in the following form:

$$h_c(\tau) = h_c(t)e^{2i\pi[\phi'(t)(\tau-t)+\frac{1}{2}\phi''(t)(\tau-t)^2]}. \tag{33}$$

Then, we have the following result.

Proposition 1. *The STFT of h_c, computed using the Gaussian window $g(t) = e^{-\pi t^2}$ admits the following closed-form expression:*

$$V^g_{h_c}(\eta, t) = h_c(t) r^{-\frac{1}{2}} e^{-i\frac{\theta}{2}} e^{-\frac{\pi(1+i\phi''(t))(\eta-\phi'(t))^2}{1+\phi''(t)^2}}. \tag{34}$$

Proof. We remark that

$$V^g_{h_c}(\eta, t) \;=\; h_c(t)\mathcal{F}\{e^{-\pi(1-i\phi''(t))\tau^2}\}(\eta - \phi'(t)) = h_c(t)\widehat{e^{-\pi z\tau^2}}(\eta - \phi'(t)),$$

where $z = 1 - i\phi''(t) = re^{i\theta}$. Lemma 1 then gives

$$V^g_{h_c}(\eta, t) = h_c(t) z^{-\frac{1}{2}} e^{-\pi\frac{(\eta-\phi'(t))^2}{z}} = h_c(t) z^{-\frac{1}{2}} e^{-\pi\frac{(\eta-\phi'(t))^2}{r}} e^{-i\theta}. \tag{35}$$

□

From this, we immediately get that:

$$\hat{\omega}_{h_c}(\eta,t) - \phi'(t) = \frac{\phi''(t)^2}{1+\phi''(t)^2}(\eta - \phi'(t)). \tag{36}$$

This shows that the IF estimate is not exact for linear chirp. So now, if $|\eta - \phi'(t)| < \varepsilon$, we obtain:

$$|\hat{\omega}_{h_c}(\eta,t) - \phi'(t)| < \varepsilon |1 - \frac{1}{1+\phi''(t)^2}|.$$

Here we see that the quality of the estimate $\widehat{\omega}_{h_c}(\eta,t)$ close to the curve $(t,\phi'(t))$ only depends on the magnitude of $\phi''(t)$: if the latter goes to zero, the estimate tends to $\phi'(t)$. This justifies why, in Theorem 1, we assume the modes satisfy $\phi''(t) \leq \varepsilon$: what matters is how small the modulation is, $\phi'(t)$ playing no role.

4. New FSST based on second order approximation of the phase

The original FSST assumes $\phi''(t)$ is negligible but, in many situations, the signal exhibits high frequency modulation, which reduces the applicability of the results of Theorems 1 and 3. Many different approaches have been carried out to take into account the modulation in the synchrosqueezing context, as for instance by introducing a demodulation operator before applying the synchrosqueezing transform [13] [20]. In another direction, an extension of FSST, based on a second order approximation of the phase, was recently proposed in [16], but, to our knowledge, no theoretical analysis of the proposed estimate is available. We propose to bridge that gap in this section.

4.1. Computation of the new IF estimate

Remember $\tilde{\omega}_f(\eta,t) = \frac{\partial_t V_f^g(\eta,t)}{2i\pi V_f^g(\eta,t)}$ and then introduce:

$$\tilde{t}_f(\eta,t) \;\; = \;\; t - \frac{\partial_\eta V_f^g(\eta,t)}{2i\pi V_f^g(\eta,t)}. \tag{37}$$

Similarly to $\widehat{\omega}_f(\eta,t) = \mathcal{R}(\tilde{\omega}_f(\eta,t))$, we define $\widehat{t}_f(\eta,t) = \mathcal{R}(\tilde{t}_f(\eta,t))$. First, we recall an estimate of the frequency modulation introduced in [16].

Definition 5. *Let $f \in L^2(\mathbb{R})$ and consider when $V_f^g(\eta,t) \neq 0$ and $\partial_t \left(\frac{\partial_\eta V_f^g(\eta,t)}{V_f^g(\eta,t)} \right) \neq 2i\pi$ the quantity*

$$\tilde{q}_f(\eta,t) = \frac{\partial_t \tilde{\omega}_f(\eta,t)}{\partial_t \tilde{t}_f(\eta,t)} = \frac{\partial_t \left(\frac{\partial_t V_f^g(\eta,t)}{V_f^g(\eta,t)} \right)}{2i\pi - \partial_t \left(\frac{\partial_\eta V_f^g(\eta,t)}{V_f^g(\eta,t)} \right)}. \tag{38}$$

An estimate of the frequency modulation is then defined by

$$\hat{q}_f(\eta,t) = \mathcal{R}\left(\tilde{q}_f(\eta,t)\right). \tag{39}$$

Here we propose to focus on the study of IF estimate associated with TF representation given by STFT. In this regard, we study a slightly different IF estimate from the one introduced in [16], which allows for mathematical study.

Definition 6. *Let $f \in L^2(\mathbb{R})$, we define the second order IF complex estimate of f as:*

$$\tilde{\omega}_f^{(2)}(\eta,t) = \begin{cases} \tilde{\omega}_f(\eta,t) + \tilde{q}_f(\eta,t)(t - \tilde{t}_f(\eta,t)) & \text{if } \partial_t \tilde{t}_f(\eta,t) \neq 0 \\ \tilde{\omega}_f(\eta,t) & \text{otherwise,} \end{cases} \tag{40}$$

and then its real part $\hat{\omega}_f^{(2)}(\eta,t) = \mathcal{R}(\tilde{\omega}_f^{(2)}(\eta,t))$.

Remark 7. The estimate (39) was used in [16] where it was proved that $\hat{q}_f(\eta,t) = \phi''(t)$, when f is a Gaussian modulated linear chirp, i.e. a chirp where both ϕ and $\log(A)$ are quadratic. Further, a new estimate of $\phi'(t)$ was also derived there, namely:

$$\phi'(t) \approx \widehat{\omega}_f(\eta,t) + \hat{q}_f(\eta,t)(t - \hat{t}_f(\eta,t)), \tag{41}$$

which is exact for constant amplitude linear chirp.

Proposition 2. *Let $f \in L^2(\mathbb{R})$, then the IF estimate $\widehat{\omega}_f^{(2)}(\eta,t)$ can be expressed by means of five different STFTs, since we have:*

$$\begin{aligned} \tilde{\omega}_f(\eta,t) &= \eta - \frac{1}{2i\pi} \frac{V_f^{g'}(\eta,t)}{V_f^g(\eta,t)}, \\ \tilde{q}_f(\eta,t) &= \frac{1}{2i\pi} \frac{V_f^{g''}(\eta,t) V_f^g(\eta,t) - (V_f^{g'}(\eta,t))^2}{V_f^{tg}(\eta,t) V_f^{g'}(\eta,t) - V_f^{tg'}(\eta,t) V_f^g(\eta,t)}, \\ t - \tilde{t}_f(\eta,t) &= -\frac{V_f^{tg}(\eta,t)}{V_f^g(\eta,t)}. \end{aligned}$$

Proof. The expressions for $\tilde{\omega}_f(\eta,t)$ and $t-\tilde{t}_f(\eta,t)$ are straightforward. Indeed, since g is in the Schwartz class, the STFT of f belongs to $C^\infty(\mathbb{R})$, and we have:

$$\begin{aligned}\partial_\eta V_f^g(\eta,t) &= -2i\pi V_f^{tg}(\eta,t)\\ \partial_t V_f^g(\eta,t) &= 2i\pi\eta V_f^g(\eta,t) - V_f^{g'}(\eta,t).\end{aligned} \tag{42}$$

Based on these equalities, the expression for $\tilde{q}_f(\eta,t)$ is easy to obtain. □

In the following section, we use IF estimate $\hat{\omega}_f^{(2)}(\eta,t)$ to define a new synchrosqueezing transform for which we prove approximation results.

Remark 8. It is worth noticing here that by exploiting the properties of STFT regarding derivation, Proposition 2 tells us that one does not need to use finite differences to compute $\tilde{q}_f(\eta,t)$ and $\tilde{\omega}_f(\eta,t)$.

4.2. Definition of the new FSST and approximation results

In this section, we define another class of chirp-like functions larger than $\mathcal{B}_{\Delta,\varepsilon}$ and show that they can be successfully dealt with by means of second order FSST, which is defined in this section. So first, we define the new set of multicomponent signals we are studying:

Definition 7. *Let $\varepsilon>0$ and $\Delta>0$. The set $\mathcal{B}^{(2)}_{\Delta,\varepsilon}$ of multicomponent signals with second order modulation ε and separation Δ corresponds to the signals defined in* (7) *satisfying:*

(a) function f_k is such that A_k and ϕ_k satisfy the following conditions:

$$\begin{gathered}A_k(t)\in L^\infty(\mathbb{R})\cap C^2(\mathbb{R}),\ \phi_k(t)\in C^3(\mathbb{R}),\\ \phi_k'(t),\ \phi_k''(t),\ \phi_k'''(t)\in L^\infty(\mathbb{R}),\\ A_k(t)>0,\ \inf_{t\in\mathbb{R}}\phi_k'(t)>0,\ \sup_{t\in\mathbb{R}}\phi_k'(t)<\infty,\\ |A_k'(t)|\le\varepsilon,\ |A_k''(t)|\le\varepsilon,\ \text{and } |\phi_k'''(t)|\le\varepsilon,\end{gathered}$$

(b) functions f_ks satisfy the following separation condition

$$\phi_{k+1}'(t)-\phi_k'(t)>2\Delta,\quad \forall t\in\mathbb{R}\ \ ,\ \ \forall k\in\{1,\cdots,K-1\}. \tag{43}$$

Now, let us define the second order FSST as follows

Definition 8. *Let h be a positive L^1-normalized window belonging to $C_c^\infty(\mathbb{R})$, and consider $\gamma, \lambda > 0$, the second order FSST of f with threshold γ and accuracy λ is defined by:*

$$\widetilde{T}_f^{\lambda,\gamma}(\omega,t) = \frac{1}{g(0)} \int_{|V_f^g(\eta,t)|>\gamma} V_f^g(\eta,t) \frac{1}{\lambda} h\left(\frac{\omega - \hat{\omega}_f^{(2)}(\eta,t)}{\lambda}\right) d\eta. \tag{44}$$

In Section 3, we showed that, for functions $f \in \mathcal{B}_{\Delta,\varepsilon}$, a good IF estimate was given by $\hat{\omega}_f(\eta,t)$ and the approximation theorem followed. Here, to assess the approximation property of the second order FSST we have just introduced, we consider a function $f \in \mathcal{B}_{\Delta,\varepsilon}^{(2)}$ for which we are going to prove that a good IF estimate is provided by $\hat{\omega}_f^{(2)}(\eta,t)$. The approximation theorem is as follows:

Theorem 4. *Consider $f \in \mathcal{B}_{\Delta,\varepsilon}^{(2)}$, set $\tilde{\varepsilon} = \varepsilon^{1/6}$. Let g be a window satisfying, for all t, all $k = 1, \cdots, K$ and $r \in \{0,1,2\}$ that, if $|\eta| \geq \Delta$, $|\mathcal{F}\{\tau^r g(\tau) e^{i\pi\phi_k''(t)\tau^2}\}(\eta)| \leq K_r \varepsilon$, where K_r is some constant. Furthermore if, for all $k = 1, \cdots, K$, $\int_{|\eta|>\Delta} |\mathcal{F}\{g(\tau) e^{i\pi\phi_k''(t)\tau^2}\}(\eta)| d\eta \leq K_3 \tilde{\varepsilon}$, for some constant K_3, then, provided ε is sufficiently small, the following hold:*

(a) $|V_f^g(\eta,t)| \geq \tilde{\varepsilon}$ only when there exists $k \in \{1, ..., K\}$ such that $(\eta,t) \in Z_k$.

(b) For all $k \in \{1, ..., K\}$ and all $(\eta,t) \in Z_k$ such that $|V_f^g(\eta,t)| > \tilde{\varepsilon}$ and $|\partial_t \tilde{t}_f(\eta,t)| > \tilde{\varepsilon}$ we have

$$|\widehat{\omega}_f^{(2)}(\eta,t) - \phi_k'(t)| \leq \tilde{\varepsilon}. \tag{45}$$

(c) Moreover, for each $k \in \{1, ..., K\}$, there exists a constant D such that

$$\left| \left(\lim_{\lambda \to 0} \int_{\mathcal{M}_{k,\tilde{\varepsilon}}} \widetilde{T}_f^{\lambda,\tilde{\varepsilon}}(\omega,t) d\omega \right) - f_k(t) \right| \leq D\tilde{\varepsilon}, \tag{46}$$

where $\mathcal{M}_{k,\tilde{\varepsilon}} := \{\omega : |\omega - \phi_k'(t)| < \tilde{\varepsilon}\}$, provided the Lebesgue measure $\mu\{\eta,\ s.t.(\eta,t)\ \in Z_k, |\partial_t \tilde{t}_f(\eta,t)| \leq \tilde{\varepsilon}\} \leq \gamma\tilde{\varepsilon}$ for some constant γ.

The proof of this Theorem is available in Section Appendix.

Remark 9. The assumption $|\eta| > \Delta \Rightarrow |\mathcal{F}\{g(\tau)e^{i\pi\phi_k''(t)\tau^2}\}(\eta)| \leq K_0\varepsilon$ is somewhat complex, so we try here to explain what it really means. Let us fix the ridge number k and set $c = \phi_k''(t)$, the assumption ensures a sufficient decrease of the Fourier transform of:

$$l(\tau) = g(\tau)e^{i\pi c\tau^2}.$$

For a Gaussian window, $g(t) = e^{-\pi t^2}$, $\hat{l}$ has the following closed-form expression:

$$|\hat{l}(\eta)| = \left(1 + c^2\right)^{-\frac{1}{4}} e^{\frac{-\pi}{1+c^2}\eta^2}.$$

It is clear that, if we take Δ large enough, we achieve the assumption. When g is not a Gaussian function, we cannot compute $\hat{l}$, but can still perform an estimation of the decay of $|\hat{l}|$ by means of the stationary phase approximation: the phase within the integral

$$\hat{l}(\eta) = \int_{\mathbb{R}} g(\tau)e^{i\pi c\tau^2}e^{-2i\pi\eta\tau}\,d\tau$$

admits a stationary point at $\tau_c = \frac{\eta}{c}$. The stationary phase theorem finally gives

$$|\hat{l}(\eta)| \approx \frac{1}{\sqrt{|c|}}\left|g\left(\frac{\eta}{c}\right)\right|.$$

Again, by assuming Δ large enough, one can satisfy the assumption. Now, if we consider all the ridges together, things are more complex, since choosing a large Δ implies the ridges need to be farther apart. But this is something that is expected: the frequency modulation makes the frequency support of the TF response associated with one mode larger, thus it changes the separation condition. In practice, the window's choice is driven by this trade-off between separation and localization.

4.3. Second order synchrosqueezing in the CWT framework

It is still possible to define a second order IF estimate, in the wavelet framework, by putting $\tilde{t}_f(a,t) := \frac{\int_{\mathbb{R}} \tau f(\tau)\frac{1}{a}\psi(\frac{\tau-t}{a})^* d\tau}{W_f^\psi(a,t)}$, $\tilde{q}_f(a,t) = \frac{\partial_t\tilde{\omega}_f(a,t)}{\partial_t\tilde{t}_f(a,t)}$, and then defining:

Definition 9.

$$\tilde{\omega}_f^{(2)}(a,t) \;=\; \begin{cases} \tilde{\omega}_f(a,t) + \tilde{q}_f(a,t)(t - \tilde{t}_f(a,t)) & \text{if } \partial_t \tilde{t}_f(a,t) \neq 0 \\ \tilde{\omega}_f(a,t) & \text{otherwise,} \end{cases} \tag{47}$$

and then its real part $\hat{\omega}_f^{(2)}(a,t) = \mathcal{R}(\tilde{\omega}_f^{(2)}(a,t))$.

Then, to define a second order synchrosqueezing operator in the wavelet case is straightforward: we just replace the IF estimate $\hat{\omega}_f$ by $\hat{\omega}_f^{(2)}$. Unfortunately, its theoretical analysis cannot be directly derived from the just studied STFT framework, therefore it is left for future work.

5. Numerical Results

In order to illustrate the behavior of our new second order synchrosqueezing transform, we apply it to the same test signals as in [16]. One (signal 1) is made of low-order polynomial chirps, that behave locally as linear chirps, and the other one (signal 2) contains strongly nonlinear sinusoidal frequency modulations. We will compare the results of the FSST (first-order STFT-based SST) and the new second-order synchrosqueezing transform, designed by VSST. We choose this denomination after the so-called VSST technique which is the other transform based on the second order approximation of the phase, which was introduced in [16]. Figure 1 shows the STFT, FSST, and new VSST for both test-signals 1 and 2. Note that in our simulations, we used 1024 time samples over $[0, 1]$ and a Gaussian window of size 400. For reproducibility purposes, the Matlab code for VSST, as well as the scripts generating all the Figures of this paper, can be downloaded from `http://oberlin.perso.enseeiht.fr/files/vsst.zip`.

5.1. Quality of representation

In order to quantify the quality of the representation given by the new VSST, we propose to measure the amount of information contained in the coefficients with the largest amplitude. In this regard, one way to compare the different transformations is to compute the normalized energy associated with the first coefficients with the largest amplitude: the faster the growth of this energy towards 1, the sharper the representation. In Fig. 2 A and

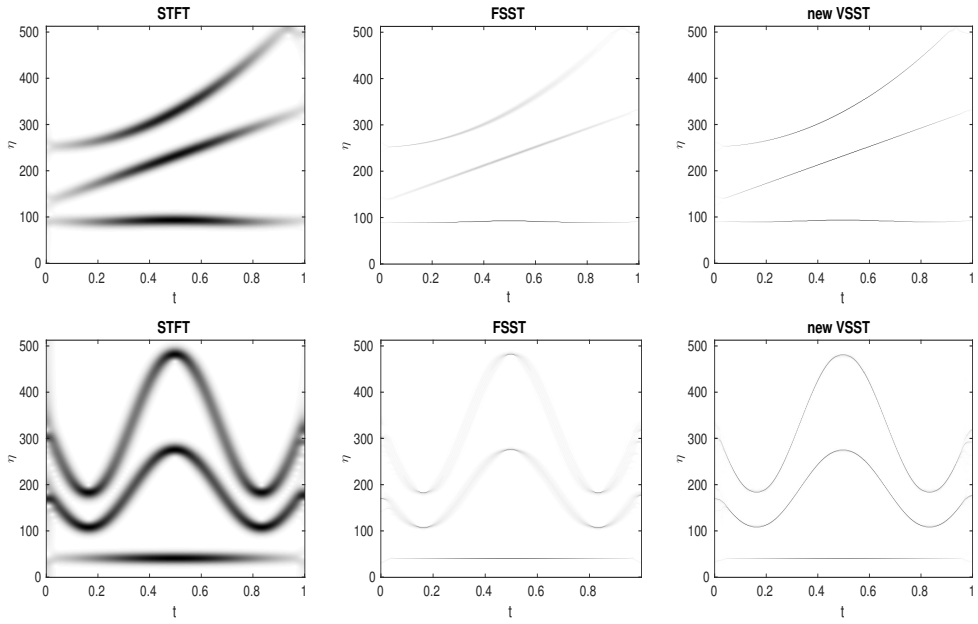

Figure 1: first row: magnitude of STFT, FSST and new VSST for test-signal 1; second row: same computation but for test-signal 2

B, these normalized energies are displayed with respect to the number of coefficients kept divided by the length of the signal, for both test-signals, and for the three representations, namely VSST proposed in [16], new VSST and FSST. In our context, the normalized energy is computed as the cumulative sum of the squared sorted coefficients over the sum of all the squared coefficients. The first remark is that both VSST and new VSST behave similarly for test-signal 1 while slightly better results are obtained when the latter is used on test-signal 2, which contains stronger frequency modulations. The second remark is that one needs only 3 coefficients per time instant to recover the signal energy, which is consistent with the three modes making up the test-signal. In order to investigate the influence of noise on the sparsity of the representation, we carry out the same experiments when the test-signals are contaminated by white Gaussian noise (noise level 0 dB). The results displayed on Fig. 2 C and D exhibit a slower increase of the normalized energy, since the coefficients corresponding to noise are spread over the whole TF plane. However, our proposed new VSST still behaves better than both VSST and FSST in this noisy situation.

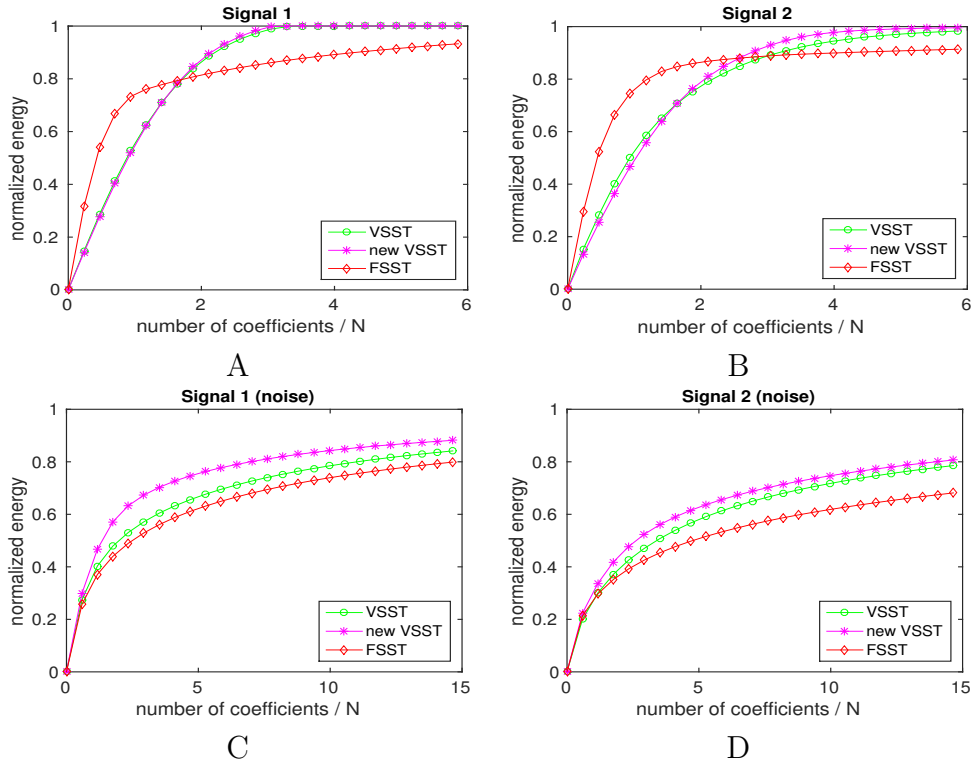

Figure 2: Normalized energy as a function of the number of sorted coefficients for test-signals 1 (A) and 2 (B). Abscissa gives the number of coefficients kept over the length N of the signal, i.e., the mean number of coefficients kept in each column of the TF plane. C and D: idem as A and B but for noisy signals (0 dB).

To better evaluate the quality of the TF representation, we will compare the obtained representation and the ideal one, by means of the Earth mover's distance (EMD) [17]. EMD is a sliced (fixed time) Wasserstein distance aimed at comparing probability distributions, that has been already used in the time-frequency context by [10, 24]. We will compare our new VSST technique with FSST, and with the recently proposed synchrosqueezed wave packet transform (SSWPT) [24]. This last technique has proven to be more robust to noise than standard synchrosqueezing transform, because it makes use of redundancy of the wave packet decomposition. We will also compared the obtained representation with the reassignment method (RM) [1], which behaves well with frequency modulation, but does not allow for reconstruction.

To clearly state the interest of the new VSST we introduced, we investigate the quality of representation associated with the middle mode of test-signal 2, which exhibits relatively high frequency modulation (the sampling frequency is 1024 Hz). The results depicted in Figure 3 show the benefits of taking the modulation into account, since RM and new VSST behave much better than the other methods at low noise levels. Also, at very high noise levels, the method based on wavelet packet transform provides with a more accurate TF representation, but the new VSST remains always better that FSST even in these configurations. An alternative technique, called *ConceFT*

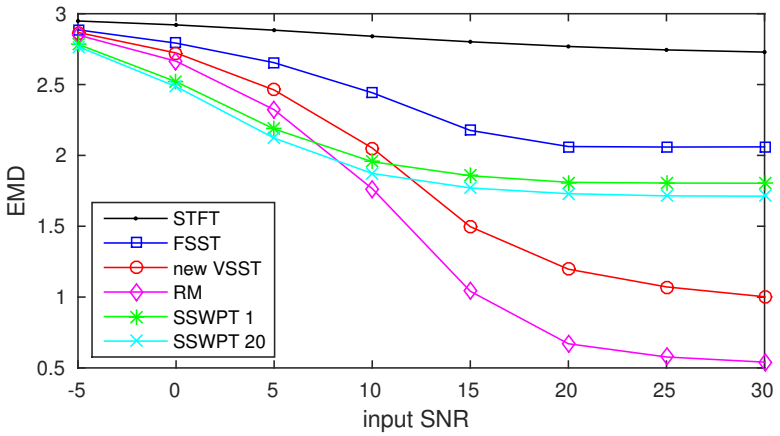

Figure 3: Comparison of the quality of the TF representations either given by STFT, FSST, RM, VSST, SSWPT (for redundancy factor red = 1 or 20), for the highest frequency mode of test-signal 2

was recently proposed in [10] and consists in using a multi-taper approach in the WSST framework, a technique first introduced in [23] in the context of spectrogram reassignment. In a nutshell, the approach aims to improve the TF representation associated with the synchrosqueezing using a single wavelet by averaging WSSTs associated with linear combinations of orthogonal wavelets. In many situations, this approach results in a significant part of the noise being removed. However, since it relies on transforms that do not explicitly take into account the modulation, the results are not satisfactory when applied to signals where the former is important. In this regard, we believe that it would be of interest to design a new version of ConceFT whose block basis would be our second order SST rather than a wavelet transform,

but this is left for future investigation.

5.2. Choice of the window

The choice of the window's length is a critical step for any time-frequency representation. A careful study of the approximation theorem of first-order SST shows that the window should be taken small enough, to minimize the estimation error; and large enough to satisfy the separation condition between the different modes. In practice, one needs to tune the window's length to achieve a trade-off between *localization* and *separation*.

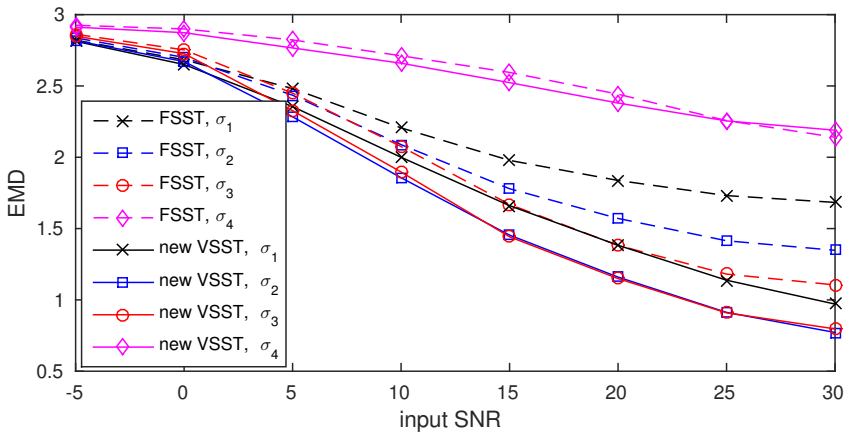

Figure 4: Comparison of the quality of the TF representations given by FSST and VSST, with 4 different windows.

In the VSST case, the window must still be chosen so as to satisfy the separation condition between modes. But, since it uses a second-order approximation of the phase, VSST does not require a small window to produce a concentrated representation. This phenomenon is illustrated in the following Figure 4, which displays the EMD with respect to the input SNR for the same signal as in Figure 3. It compares FSST and VSST, computed with a Gaussian window with 4 significant values of σ ranked increasingly, meaning that to choose σ outside $[\sigma_1, \sigma_4]$ leads to worse results. It is clear that for a given σ, VSST always considerably improves the results. Moreover, the performance of FSST for the optimal window σ_3 is significantly worse than the result provided by VSST. Finally, both σ_2 and σ_3 give accurate results

for VSST, showing that the window's choice with our method is less critical than with FSST.

To better illustrate the influence of the window, we show in Figure 5 the results of FSST and VSST for window's sizes σ_3 and σ_4. We remark that for σ_3, which is the optimal parameter for FSST, the latter does not give a very sharp representation and, taking a larger value, as for instance σ_4, results in strong inter-mode interference.

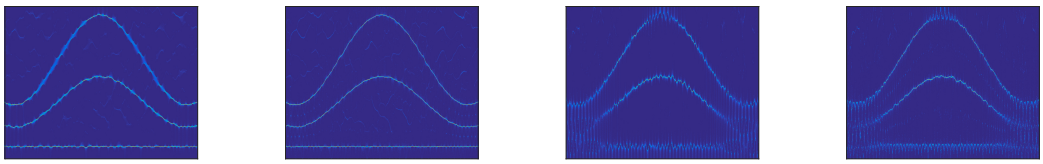

FSST, σ_3 VSST, σ_3 FSST, σ_4 VSST, σ_4

Figure 5: Comparison between FSST and VSST, with two different window's sizes ($\sigma_3 < \sigma_4$).

5.3. Reconstruction of the modes

The main advantage of synchrosqueezing techniques over traditional reassignment techniques lies in its invertibility. To improve the accuracy of the reassignment step in synchrosqueezing techniques by using new VSST naturally leads to better reconstruction results. The reconstruction formula used to retrieve the kth mode, assuming $\hat{\phi}'_k(t)$ is an estimate of $\phi'_k(t)$, is as follows:

$$f_k(t) \approx \int_{|\omega - \hat{\phi}'_k(t)| < d} T_f(\omega, t) d\omega, \tag{48}$$

as explained in more details in [16]. The parameter d is here to compensate for the fact that $\hat{\phi}'_k(t)$ is an estimate of $\phi'_k(t)$ and not the true value. Provided d is of the same order of magnitude as the estimation error, this reconstruction formula ensures an asymptotically perfect reconstruction. To compute an estimation of the ridges $(t, \phi'_k(t))_k$, knowing the number K of modes, we use the algorithm introduced in [3], which computes a local minimum of the functional:

$$E_f((\varphi_k)_{k=1,\cdots,K}) = \sum_{k=1}^{K} - \int_{\mathbb{R}} |T_f(t, \varphi_k(t))|^2 dt + \int_{\mathbb{R}} (\lambda \varphi'_k(t)^2 + \beta \varphi''_k(t)^2) dt, \tag{49}$$

λ and β being two positive tuning parameters. Then $(\hat{\phi}'_k(t))_{k=1,\cdots,K} = \operatorname{argmin} E_f((\varphi_k)_{k=1,\cdots,K})$. In practice, we notice that since the TF representation given by the second order synchrosqueezing is very well concentrated, the choice for regularization parameters is not essential.

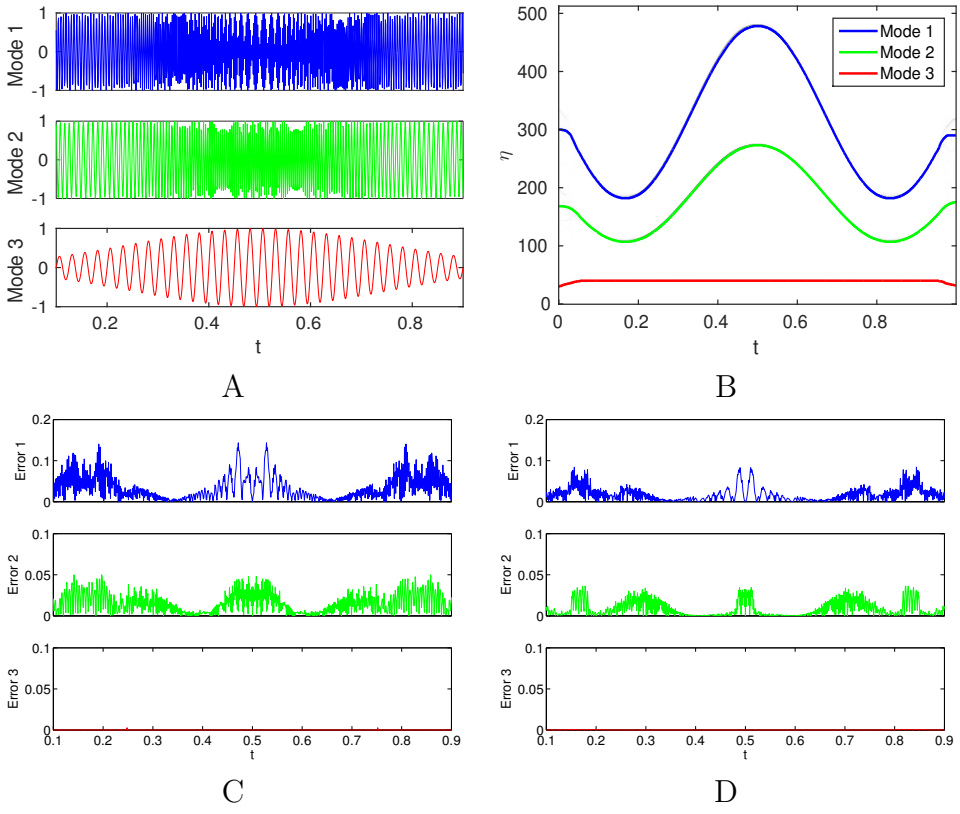

Figure 6: A: Mode retrieval based on new VSST for test-signal 2; B: Estimated ridges superimposed on the new VSST of test-signal 2. We use $d = 5$ in the reconstruction, and $\beta = 0, \lambda = 0.02$ for the ridge extraction; C: Reconstruction errors associated with each mode of test-signal 2 using old VSST D: Same as C but with the new VSST

To illustrate the behavior of our new VSST technique, we first display the reconstruction process associated with test-signal 2 in Figure 6 A, the ridges used for reconstruction being depicted in Figure 6 B. Then, to compare the proposed new VSST with the alternative technique proposed in [16], we display, in Figure 6 C and D, the reconstruction error at each time instant for the three modes and for both VSST and new VSST. The improvement

brought by using new VSST instead of old VSST appears to be the most significant when the modulation is strong (i.e., in the mode associated with the highest frequency in the studied case). Compared to the same figure plotted for FSST in [16], the error is really decreased.

To further quantify the accuracy of mode reconstruction in noisy situations, we investigate the output SNR for test-signal 2 as a function of input SNR. The proposed comparison involves FSST and new VSST and the computation is performed for two different values of parameter d, using the true instantaneous frequencies to avoid dependency on the ridge detection step. It is worth mentioning here that parameter d enables the error associated with IF estimation with the different techniques to be compensated for. Indeed, to get good reconstruction results, d needs to be all the larger that the IF estimate is inaccurate. Also, a larger d still compatible with the separation condition on the modes, will also mean better reconstruction results. These facts are numerically illustrated in Figure 7 where, for a fixed d, the reconstruction results is always better with new VSST than with FSST, and where, for a given method, the quality of the reconstruction is improved by choosing a larger d. Also, one remarks that whatever the value of d, the reconstruction given by SST reaches a step and does not increase after some input SNR. This is because even with no noise, the SST can not reach a very high reconstruction due to the bad IF estimate.

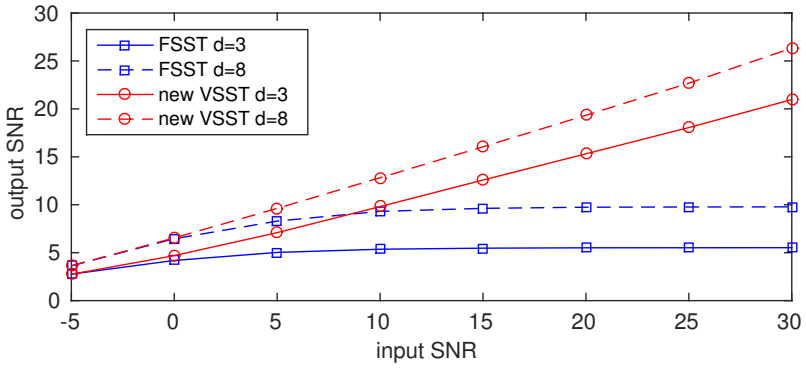

Figure 7: comparison of the quality of the mode reconstruction either given by FSST or new VSST (for two different values of parameter d and for test-signal 2), measured by output SNR with respect to input SNR

6. Conclusion

In this paper, we developed a novel synchrosqueezing transform for analyzing multicomponent signals made of strongly frequency-modulated modes, based on the short-time Fourier transform. It simply consists in a refinement of the instantaneous frequency estimate, computed using a second-order expansion of the phase. After having revisited the case of first-order synchrosqueezing, releasing the hypothesis of a window compactly supported in the frequency domain, we proved a novel approximation theorem involving the proposed new synchrosqueezing transform applied to multicomponent signals made of strongly modulated modes. Numerical experiments showed the benefits of taking into account frequency modulation for both representation and reconstruction purposes. Interestingly, the new transformation has proven to be quite robust against noise and exhibits less sensitivity to the window's choice. A limitation of the proposed theoretical study is that it is restricted to modes with small amplitude modulations, and to improve this aspect is a work currently underway.

Acknowledgement

The authors acknowledge the support of the French Agence Nationale de la Recherche (ANR) under grant ANR-13-BS03-0002-01.

Appendix

The proof of Theorem 4 involves a number of estimates, which are shown hereafter.

Lemma 2. *For any (η, t), there is at most one $k \in \{1, \cdots, K\}$ for which $|\eta - \phi_k'(t)| \leq \Delta$.*

The proof is straightforward and is left to the reader. For our purpose, we need to analyze the behavior of the STFT on a linear chirp, for which we have the following proposition.

Proposition 3. *Let $h(\tau) = Ae^{2i\pi\phi(\tau)}$ be a linear chirp and consider $V_h^{t^r g}$, for $r \in \{0, 1, 2\}$, the STFT of h obtained with a window $t^r g$, where g satisfies the hypotheses of Theorem 4. If $|\eta - \phi'(t)| > \Delta$ then*

$$|V_h^{t^r g}(\eta, t)| \leq \varepsilon K_r A.$$

Proof. We know that $V_h^{t^r g}(\eta,t) = h(t)\mathcal{F}\{\tau^r g(\tau)e^{i\pi\phi''(t)\tau^2}\}(\eta-\phi'(t))$ so that, if $|\eta-\phi'(t)|>\Delta$, assumptions on g lead to $|V_h^{t^r g}(\eta,t)| \leq \varepsilon K_r A$. □

Proposition 4. *For any $k\in\{1,\cdots,K\}$, any $r\in\{0,1,2\}$, and any $(\eta,t)\notin Z_k$, we have:*

$$|V_{f_k}^{t^r g}(\eta,t)| \leq \varepsilon E_{k,r}(t), \tag{50}$$

with $E_{k,r}(t) = I_{r+1} + (\frac{\pi}{3}I_{r+3} + K_r)A_k(t)$. Consequently, for any $(\eta,t)\in Z_k$:

$$|V_f^{t^r g}(\eta,t) - V_{f_k}^{t^r g}(\eta,t)| \;\leq\; \varepsilon\sum_{l\neq k} E_{l,r}(t) := \varepsilon\Omega_{k,r}(t), \tag{51}$$

Proof. First, we write

$$\begin{aligned}
f_k(\tau) &= A_k(\tau)e^{2i\pi\phi_k(\tau)} = (A_k(\tau)-A_k(t))e^{2i\pi\phi_k(\tau)}\\
&+ A_k(t)e^{2i\pi[\phi_k(t)+\phi_k'(t)(\tau-t)+\frac{1}{2}\phi_k''(t)(\tau-t)^2]}\\
&+ A_k(t)[e^{2i\pi[\phi_k(t)+\phi_k'(t)(\tau-t)+\frac{1}{2}\phi_k''(t)(\tau-t)^2+\frac{1}{2}\int_t^\tau \phi_k'''(x)(\tau-x)^2dx]} - e^{2i\pi[\phi_k(t)+\phi_k'(t)(\tau-t)+\frac{1}{2}\phi_k''(t)(\tau-t)^2]}]\\
&= f_{k,1}(\tau)+f_{k,2}(\tau)+f_{k,3}(\tau).
\end{aligned} \tag{52}$$

Then, for any (η,t),

$$\begin{aligned}
|V_{f_{k,1}}^{t^r g}(\eta,t)| &\leq \int_{\mathbb{R}} |A_k(\tau)-A_k(t)||\tau-t|^r|g(\tau-t)|d\tau,\\
&\leq \int_{\mathbb{R}} \varepsilon|\tau-t|^{r+1}|g(\tau-t)|d\tau \leq \varepsilon I_{r+1},
\end{aligned}$$

and

$$\begin{aligned}
|V_{f_{k,3}}^{t^r g}(\eta,t)| &\leq \pi A_k(t)\int_{\mathbb{R}}\left(\int_t^\tau |\phi'''(x)||\tau-x|^2\,dx\right)|\tau-t|^r|g(\tau-t)|\,d\tau\\
&\leq \frac{\pi}{3}A_k(t)\int_{\mathbb{R}}\varepsilon|\tau-t|^{r+3}|g(\tau-t)|\,d\tau\\
&\leq \frac{\pi}{3}A_k(t)\varepsilon I_{r+3}.
\end{aligned}$$

Using Proposition 3, we get (50), and inequality (51) follows. □

Now, if $(\eta,t)\notin \bigcup_{l=1}^K Z_l$, we immediately get:

$$|V_f^g(\eta,t)| \leq \varepsilon\sum_{l=1}^K E_{l,0}(t) \leq \tilde{\varepsilon},$$

when $\tilde{\varepsilon}$ is sufficiently small, which proves item (a) of Theorem 4.
Now, we introduce several propositions that are useful to prove item (b) of Theorem 4.

Proposition 5. *For any $(\eta, t) \in Z_k$, assuming g satisfies the hypotheses of Theorem 4, we have:*

$$\left|\partial_t V_f^g(\eta,t) - 2i\pi\left(\phi_k'(t)V_f^g(\eta,t) + \phi_k''(t)V_f^{tg}\right)\right| \leq \varepsilon B_{k,1}(t), \tag{53}$$

where

$$\begin{aligned} B_{k,1}(t) &= KI_0 + \sum_{k=1}^{K} \|A_k\|_\infty \pi I_2 + 2\pi \sum_{l\neq k} (\phi_l'(t)E_{l,0}(t) + |\phi_l''(t)|E_{l,1}(t)) \\ &\quad + 2\pi(\phi_k'(t)\Omega_{k,0}(t) + |\phi_k''(t)|\Omega_{k,1}(t)) \end{aligned}$$

Proof. Differentiating the STFT of f with respect to t, we get for any (η, t):

$$\begin{aligned} \partial_t V_f^g(\eta,t) &= \sum_{k=1}^{K} \int_{\mathbb{R}} A_k'(\tau) e^{2i\pi\phi_k(\tau)} g(\tau-t) e^{-2i\pi\eta(\tau-t)} d\tau \\ &+ \sum_{k=1}^{K} \int_{\mathbb{R}} A_k(\tau) 2i\pi\phi_k'(\tau) e^{2i\pi\phi_k(\tau)} g(\tau-t) e^{-2i\pi\eta(\tau-t)} d\tau \\ &= \sum_{k=1}^{K} \int_{\mathbb{R}} A_k'(\tau) e^{2i\pi\phi_k(\tau)} g(\tau-t) e^{-2i\pi\eta(\tau-t)} d\tau \\ &+ \sum_{k=1}^{K} \int_{\mathbb{R}} A_k(\tau) 2i\pi \left[\phi_k'(t) + (\tau-t)\phi_k''(t) + \int_t^\tau (\tau-u)\phi_k'''(u)du\right] e^{2i\pi\phi_k(\tau)} g(\tau-t) e^{-2i\pi\eta(\tau-t)} d\tau \\ &= \sum_{k=1}^{K} \int_{\mathbb{R}} A_k'(\tau) e^{2i\pi\phi_k(\tau)} g(\tau-t) e^{-2i\pi\eta(\tau-t)} d\tau + \sum_{k=1}^{K} 2i\pi\phi_k'(t) V_{f_k}^g(\eta,t) \\ &+ \sum_{k=1}^{K} 2i\pi\phi_k''(t) V_{f_k}^{tg}(\eta,t) \\ &+ \sum_{k=1}^{K} \int_{\mathbb{R}} A_k(\tau) 2i\pi \left(\int_t^\tau (\tau-u)\phi_k'''(u)du\right) e^{2i\pi\phi_k(\tau)} e^{-2i\pi\eta(\tau-t)} g(\tau-t) d\tau. \end{aligned}$$

We may then write:

$$\begin{aligned}
&\left|\partial_t V_f^g(\eta,t) - 2i\pi \sum_{k=1}^K \left(\phi_k'(t) V_{f_k}^g(\eta,t) + \phi_k''(t) V_{f_k}^{tg}(\eta,t)\right)\right| \\
&\quad \leq \sum_{k=1}^K \int_{\mathbb{R}} |A_k'(\tau)||g(\tau-t)|d\tau + 2\pi \sum_{k=1}^K \int_{\mathbb{R}} A_k(\tau) \left(\int_t^\tau |\tau-u||\phi_k'''(u)|du\right) |g(\tau-t)|d\tau \\
&\quad \leq \varepsilon \left(K I_0 + \sum_{k=1}^K \|A_k\|_\infty \pi I_2\right).
\end{aligned}$$

From Proposition 4, we first have, when $(\eta,t) \in Z_k$:

$$\begin{aligned}
&\left|\partial_t V_f^g(\eta,t) - 2i\pi \left(\phi_k'(t) V_{f_k}^g(\eta,t) + \phi_k''(t) V_{f_k}^{tg}(\eta,t)\right)\right| \\
&\qquad \leq \varepsilon \left(K I_0 + \sum_{k=1}^K \|A_k\|_\infty \pi I_2 + 2\pi \sum_{l\neq k} (\phi_l'(t) E_{l,0}(t) + |\phi_l''(t)| E_{l,1}(t))\right),
\end{aligned}$$

and then,

$$\begin{aligned}
&\left|\partial_t V_f^g(\eta,t) - 2i\pi \left(\phi_k'(t) V_f^g(\eta,t) + \phi_k''(t) V_f^{tg}(\eta,t)\right)\right| \\
&\qquad \leq \varepsilon \left(K I_0 + \sum_{k=1}^K \|A_k\|_\infty \pi I_2 + 2\pi \sum_{l\neq k} (\phi_l'(t) E_{l,0}(t) + |\phi_l''(t)| E_{l,1}(t))\right. \\
&\qquad\quad \left. + 2\pi(\phi_k'(t)\Omega_{k,0}(t) + |\phi_k''(t)|\Omega_{k,1}(t))\right),
\end{aligned}$$

hence (53). □

Proposition 6. *For any $(\eta,t) \in Z_k$ one has:*

$$\left|\partial_{tt}^2 V_f^g(\eta,t) - 2i\pi \left(\phi_k''(t) V_f^g(\eta,t) + \phi_k'(t)\partial_t V_f^g(\eta,t) + \phi_k''(t)\partial_t V_f^{tg}(\eta,t)\right)\right| \leq \varepsilon B_{k,2}(t), \tag{54}$$

where

$$\begin{aligned}
B_{k,2}(t) = \Lambda_0 &+ 2\pi \sum_{l\neq k} (\phi_l''(t) E_{l,0}(t) + \phi_l'(t) F_{l,0}(t) + \phi''(t) F_{l,1}(t)) \\
&+ 2\pi[\phi_k''(t)\Omega_{k,0}(t) + \phi_k'(t) \sum_{l\neq k} F_{l,0}(t) + \phi_k''(t) \sum_{l\neq k} F_{l,1}(t)
\end{aligned}$$

Proof. Since, for any (η, t), one has:

$$\begin{aligned}\partial_{tt}^2 V_f^g(\eta,t) &= \sum_{l=1}^K \int_{\mathbb{R}} \left(A_l''(\tau) + 2i\pi\phi_l''(\tau)A_l(\tau) + 2i\pi\phi_l'(\tau)A_l'(\tau)\right. \\ &\qquad \left. -4\pi^2\phi_l'(\tau)^2 A_l(\tau)\right) e^{2i\pi\phi_l(\tau)} g(\tau - t) e^{-2i\pi\eta\tau - t} d\tau \\ &= \sum_{l=1}^K \int_{\mathbb{R}} A_l''(\tau) e^{2i\pi\phi_l(\tau)} g(\tau - t) e^{-2i\pi\eta(\tau - t)} d\tau \\ &\qquad + 2i\pi \sum_{l=1}^K \int_{\mathbb{R}} \phi_l''(\tau) A_l(\tau) e^{2i\pi\phi_l(\tau)} g(\tau - t) e^{-2i\pi\eta(\tau - t)} d\tau \\ &\qquad + 2i\pi \sum_{l=1}^K \int_{\mathbb{R}} \phi_l'(\tau) f_l'(\tau) g(\tau - t) e^{-2i\pi\eta(\tau - t)} d\tau,\end{aligned}$$

we have, for the first part of $\partial_{tt}^2 V_f^g(\eta, t)$,

$$\left| \sum_{l=1}^K \int_{\mathbb{R}} A_l''(\tau) e^{2i\pi\phi_l(\tau)} g(\tau - t) e^{-2i\pi\eta(\tau - t)} d\tau \right| \leq K\varepsilon I_0. \tag{55}$$

Then, for the second part of $\partial_{tt}^2 V_f^g(\eta, t)$, we may write

$$\begin{aligned}&\left| 2i\pi \sum_{l=1}^K \int_{\mathbb{R}} \phi_l''(\tau) A_l(\tau) e^{2i\pi\phi_l(\tau)} g(\tau - t) e^{-2i\pi\eta(\tau - t)} d\tau - 2i\pi \sum_{l=1}^K \phi_l''(t) V_{f_l}^g(\eta, t) \right| \\ &\quad \leq 2\pi \sum_{l=1}^K \int_{\mathbb{R}} \left(\int_t^\tau |\phi_l'''(u)| du \right) A_l(\tau) |g(\tau - t)| d\tau \\ &\quad \leq 2\pi\varepsilon \sum_{l=1}^K \|A_l\|_\infty I_1.\end{aligned}$$

Finally, we write for the third part of $\partial_{tt}^2 V_f^g(\eta, t)$, using second order Taylor expansion of $\phi_l'(\tau)$:

$$\begin{aligned}&\left| 2i\pi \sum_{l=1}^K \int_{\mathbb{R}} \phi_l'(\tau) f_l'(\tau) g(\tau - t) e^{-2i\pi\eta(\tau - t)} d\tau - 2i\pi \sum_{l=1}^K \phi_l'(t) \partial_t V_{f_l}^g(\eta, t) + \phi_l''(t) \partial_t V_{f_l}^{tg}(\eta, t) \right| \\ &= \left| 2i\pi \sum_{l=1}^K \int_{\mathbb{R}} \int_t^\tau (\tau - u) \phi_l'''(u) du \ \left(A_l'(\tau) + 2i\pi\phi_l'(\tau) A_l(\tau) \right) e^{2i\pi\phi_l(\tau)} g(\tau - t) e^{-2i\pi\eta(\tau - t)} d\tau \right| \\ &\leq \pi\varepsilon \sum_{l=1}^K (\|A_l'\|_\infty + 2\pi \|\phi_l'\|_\infty \|A_l\|_\infty) I_2.\end{aligned}$$

From this, we get:

$$\left|\partial_{tt}^2 V_f^g(\eta,t) - 2i\pi \sum_{l=1}^{K} \left(\phi_l''(t) V_{f_l}^g(\eta,t) + \phi_l'(t)\partial_t V_{f_l}^g(\eta,t) + \phi_l''(t)\partial_t V_{f_l}^{tg}(\eta,t)\right)\right| \leq \varepsilon\Lambda_0, \tag{56}$$

where $\Lambda_0 = KI_0 + 2\pi \sum_{l=1}^{K} \|A_l(t)\|_\infty I_1 + \pi \sum_{l=1}^{K} (\|A_l'\|_\infty + 2\pi\|\phi_l'\|_\infty \|A_l\|_\infty) I_2$.
Now, recalling that:

$$\begin{aligned}
|\partial_t V_{f_l}^g(\eta,t) - 2i\pi \left(\phi_l'(t) V_{f_l}^g(\eta,t) + \phi_l''(t) V_{f_l}^{tg}(\eta,t)\right)| &\leq \varepsilon \left(I_0 + \pi\|A_l\|_\infty I_2\right), \\
|\partial_t V_{f_l}^{tg}(\eta,t) - 2i\pi \left(\phi_l'(t) V_{f_l}^{tg}(\eta,t) + \phi_l''(t) V_{f_l}^{t^2 g}(\eta,t)\right)| &\leq \varepsilon (I_1 + \pi\|A_l\|_\infty I_3),
\end{aligned}$$

we may write, if $(\eta,t) \in Z_k$, and if $l \neq k$, that

$$\begin{aligned}
|\partial_t V_{f_l}^g(\eta,t)| &\leq \varepsilon \left(I_0 + \pi\|A_l\|_\infty I_2 + 2\pi(\phi_l'(t)E_{l,0}(t) + \phi_l''(t)E_{l,1}(t))\right) := \varepsilon F_{l,0}(t) \\
|\partial_t V_{f_l}^{tg}(\eta,t)| &\leq \varepsilon \left(I_1 + \pi\|A_l\|_\infty I_3 + 2\pi(\phi_l'(t)E_{l,1}(t) + \phi_l''(t)E_{l,2}(t))\right) := \varepsilon F_{l,1}(t),
\end{aligned}$$

and, finally,

$$\begin{aligned}
|\partial_t V_f^g(\eta,t) - \partial_t V_{f_k}^g(\eta,t)| &\leq \varepsilon \sum_{l\neq k} F_{l,0}(t) \\
|\partial_t V_f^{tg}(\eta,t) - \partial_t V_{f_k}^{tg}(\eta,t)| &\leq \varepsilon \sum_{l\neq k} F_{l,1}(t).
\end{aligned}$$

Using these four inequalities, we can finally write:

$$\begin{aligned}
&\left|\partial_{tt}^2 V_f^g(\eta,t) - 2i\pi \left(\phi_l''(t) V_f^g(\eta,t) + \phi_l'(t)\partial_t V_f^g(\eta,t) + \phi_l''(t)\partial_t V_f^{tg}(\eta,t)\right)\right| \\
&\qquad \leq \varepsilon \left(\Lambda_0 + 2\pi \sum_{l\neq k} (\phi_l''(t)E_{l,0}(t) + \phi_l'(t)F_{l,0}(t) + \phi''(t)F_{l,1}(t)) \right. \\
&\qquad\qquad \left. + 2\pi[\phi_k''(t)\Omega_{k,0}(t) + \phi_k'(t) \sum_{l\neq k} F_{l,0}(t) + \phi_k''(t) \sum_{l\neq k} F_{l,1}(t) \right),
\end{aligned}$$

hence the result. □

Now we can prove item (b) of Theorem 4.

Proposition 7. *For any $(\eta,t) \in Z_k$, such that $|V_f^g(\eta,t)| > \tilde{\varepsilon}$ and $|\partial_t \tilde{t}_f(\eta,t)| > \tilde{\varepsilon}$ one has:*

$$|\tilde{q}_f(\eta,t) - \phi_k''(t)| \leq \tilde{\varepsilon}. \tag{57}$$

Proof. For the sake of clarity, we omit to write (η, t) in the proof that follows:

$$
\begin{aligned}
|\phi_k''(t) - \tilde{q}_f(\eta,t)| &= \left| \phi_k''(t) - \frac{V_f^g \partial_{tt}^2 V_f^g - (\partial_t V_f^g)^2}{2i\pi (V_f^g)^2 - V_f^g \partial_{\eta t}^2 V_f^g + \partial_t V_f^g \partial_\eta V_f^g} \right| \\
&= \left| \frac{\partial_t V_f^g \left[\partial_t V_f^g + \phi_k''(t) \partial_\eta V_f^g \right]}{2i\pi (V_f^g)^2 - V_f^g \partial_{\eta t}^2 V_f^g + \partial_t V_f^g \partial_\eta V_f^g} - \frac{V_f^g \left[\partial_{tt}^2 V_f^g + \phi_k''(t) \partial_{\eta t}^2 V_f^g - 2i\pi \phi_k''(t) V_f^g \right]}{2i\pi (V_f^g)^2 - V_f^g \partial_{\eta t}^2 V_f^g + \partial_t V_f^g \partial_\eta V_f^g} \right| \\
&= \left| \frac{\partial_t V_f^g [\partial_t V_f^g - 2i\pi \phi_k''(t) V_f^{tg} - 2i\pi \phi_k'(t) V_f^g]}{2i\pi (V_f^g)^2 + 2i\pi V_f^g \partial_t V_f^{tg} - 2i\pi \partial_t V_f^g V_f^{tg}} \right| \\
&\quad + \left| \frac{V_f^g [\partial_{tt}^2 V_f^g - 2i\pi \phi_k''(t) \partial_t V_f^{tg} - 2i\pi \phi_k''(t) V_f^g - 2i\pi \phi_k'(t) \partial_t V_f^g]}{2i\pi (V_f^g)^2 + 2i\pi V_f^g \partial_t V_f^{tg} - 2i\pi \partial_t V_f^g V_f^{tg}} \right| \\
&\leq \varepsilon B_{k,1}(t) \left| \frac{\partial_t V_f^g}{2i\pi [(V_f^g)^2 + V_f^g \partial_t V_f^{tg} - \partial_t V_f^g V_f^{tg}]} \right| \\
&\quad + \varepsilon B_{k,2}(t) \left| \frac{V_f^g}{2i\pi [(V_f^g)^2 + V_f^g \partial_t V_f^{tg} - \partial_t V_f^g V_f^{tg}]} \right| \\
&\leq \tilde{\varepsilon}^3 \left(B_{k,1}(t) |\partial_t V_f^g| + B_{k,2}(t) |V_f^g| \right) \leq \tilde{\varepsilon},
\end{aligned}
$$

if $\tilde{\varepsilon}$ is sufficiently small. □

Lemma 3. *For all $k \in \{1, ..., K\}$ and any $(\eta, t) \in Z_k$ such that $|V_f^g(\eta, t)| > \tilde{\varepsilon}$ and $|\partial_t \tilde{t}_f(\eta, t)| > \tilde{\varepsilon}$, we have*

$$
|\widetilde{\omega}_f^{(2)}(\eta, t) - \phi_k'(t)| \leq \tilde{\varepsilon}. \tag{58}
$$

Proof. According to definition of $\widetilde{\omega}_f^{(2)}(\eta, t)$ in (40), we have

$$
\widetilde{\omega}_f^{(2)}(\eta, t) = \tilde{\omega}_f(\eta, t) + \tilde{q}_f(\eta, t)(t - \tilde{t}_f(\eta, t)).
$$

It follows that

$$\begin{aligned}
\left|\widetilde{\omega}_f^{(2)}(\eta,t)-\phi_k'(t)\right| &= \left|\frac{\partial_t V_f^g(\eta,t)+\tilde{q}_f(\eta,t)\partial_\eta V_f^g(\eta,t)}{2i\pi V_f^g(\eta,t)}-\phi_k'(t)\right| \\
&= \left|\frac{\partial_t V_f^g(\eta,t)-2i\pi\tilde{q}_f(\eta,t)V_f^{tg}(\eta,t)}{2i\pi V_f^g(\eta,t)}-\phi_k'(t)\right| \\
&\leq \varepsilon\frac{B_{k,1}(t)}{\left|2i\pi V_f^g(\eta,t)\right|}+\frac{|\tilde{q}_f(\eta,t)-\phi_k''(t)|\left|V_f^{tg}(\eta,t)\right|}{\left|V_f^g(\eta,t)\right|} \\
&\leq \varepsilon\frac{B_{k,1}(t)}{\left|2\pi V_f^g(\eta,t)\right|}+\tilde{\varepsilon}^3\frac{\left(B_{k,1}(t)|\partial_t V_f^g(\eta,t)|+B_{k,2}(t)|V_f^g(\eta,t)|\right)}{|V_f^g(\eta,t)|}\leq\tilde{\varepsilon}
\end{aligned}$$

when $\tilde{\varepsilon}$ is sufficiently small. □

To prove (c) of Theorem 4, is exactly the same as the proof in the weak modulation case, except that we use, at the very end of the proof, the hypothesis:

$$\left|\frac{1}{g(0)}\int_{|\eta|>\Delta}\mathcal{F}\{g(\tau)e^{i\pi\phi_l''(t)\tau^2}\}(\eta)d\eta\right|\leq\frac{K_4\tilde{\varepsilon}}{|g(0)|}\text{ for any }l,$$

and

$$\frac{1}{|g(0)|}\left|\int_{\{|\eta-\phi_k'(t)|<\Delta\}\bigcap\{\{|V_f^g(\eta,t)|\leq\tilde{\varepsilon}\}\bigcup\{|\partial_t\tilde{t}_f(\eta,t)|\leq\tilde{\varepsilon}\}\}}V_f^g(\eta,t)d\eta\right|\leq(\frac{2\Delta}{|g(0)|}+\gamma|A_k(t)|)\tilde{\varepsilon}$$

to conclude.

References

[1] Auger, F., Flandrin, P., 1995. Improving the readability of time-frequency and time-scale representations by the reassignment method. IEEE Trans. Signal Process. 43 (5), 1068–1089.

[2] Auger, F., Flandrin, P., Lin, Y., McLaughlin, S., Meignen, S., Oberlin, T., Wu, H.-T., 2013. Time-frequency reassignment and synchrosqueezing: An overview. IEEE Signal Process. Mag. 30 (6), 32–41.

[3] Carmona, R., Hwang, W., Torresani, B., 1997. Characterization of signals by the ridges of their wavelet transforms. IEEE Trans. Signal Process. 45 (10), 2586–2590.

[4] Chui, C., Lin, Y.-T., Wu, H.-T., 2016. Real-time dynamics acquisiation from irregular samples- With application to anesthesia evaluation. Anal. Appl. 14 (4), 537–590.

[5] Clausel, M., Oberlin, T., Perrier, V., 2015. The monogenic synchrosqueezed wavelet transform: a tool for the decomposition/demodulation of AM-FM images. Applied and Computational Harmonic Analysis 39 (3), 450 – 486.

[6] Costa, M., Priplata, A. A., Lipsitz, L. A., Wu, Z., Huang, N., Goldberger, A. L., Peng, C.-K., 2007. Noise and poise: enhancement of postural complexity in the elderly with a stochastic-resonance-based therapy. Europhys. Lett. EPL 77 (6), 68008.

[7] Cummings, D. A., Irizarry, R. A., Huang, N. E., Endy, T. P., Nisalak, A., Ungchusak, K., Burke, D., 2004. Travelling waves in the occurrence of dengue haemorrhagic fever in thailand. Nature 427, 344–347.

[8] Daubechies, I., Lu, J., Wu, H.-T., 2011. Synchrosqueezed wavelet transforms: An empirical mode decomposition-like tool. Appl. Comput. Harmon. Anal. 30 (2), 243–261.

[9] Daubechies, I., Maes, S., 1996. A nonlinear squeezing of the continuous wavelet transform based on auditory nerve models. Wavelets in Medicine and Biology, 527–546.

[10] Daubechies, I., Wang, Y., Wu, H.-T., 2016. Conceft: concentration of frequency and time via multitapered synchrosqueezed transform. Philosophical Transactions of the Royal Society of London A: Mathematical, Physical and Engineering Sciences 2065 (374).

[11] Huang, N., Shen, Z., Long, S., Wu, M., Shih, H., Zheng, Q., Yen, N.-C., Tung, C., Liu, H., 1998. The empirical mode decomposition and the Hilbert spectrum for nonlinear and non-stationary time series analysis. Proc. Roy. Soc. A 454, 903–995.

[12] Huang, N., Wu, Z., 2008. A review on Hilbert–Huang transform: Method and its applications to geophysical studies. Rev. Geophys. 46 (2), RG2006.

[13] Li, C., Liang, M., 2012. A generalized synchrosqueezing transform for enhancing signal time-frequency representation. Signal Processing 9 (92), 2264–2274.

[14] Meignen, S., Oberlin, T., McLaughlin, S., 2012. A new algorithm for multicomponent signals analysis based on synchrosqueezing: With an application to signal sampling and denoising. IEEE Trans. Signal Process. 60 (11), 5787–5798.

[15] Oberlin, T., Meignen, S., Perrier, V., 2014. The Fourier-based synchrosqueezing transform. In: Acoustics, Speech and Signal Processing (ICASSP). pp. 315–319.

[16] Oberlin, T., Meignen, S., Perrier, V., March 2015. Second-order synchrosqueezing transform or invertible reassignment? Towards ideal time-frequency representations. Signal Processing, IEEE Transactions on 63 (5), 1335–1344.

[17] Peleg, S., Werman, M., 2009. Fast and robust earth mover's distances. In: IEEE Int. Conf. Computer. Vision. pp. 460–467.

[18] Thakur, G., Brevdo, E., Fuckar, N., Wu, H.-T., 2013. The synchrosqueezing algorithm for time-varying spectral analysis: robustness properties and new paleoclimate applications. Signal Process. 93 (5), 1079–1094.

[19] Thakur, G., Wu, H.-T., 2011. Synchrosqueezing-based recovery of instantaneous frequency from nonuniform samples. SIAM J. Math. Analysis 43 (5), 2078–2095.

[20] Wang, S., Chen, X., Cai, G., Chen, B., Li, X., He, Z., 2014. Matching demodulation transform and synchrosqueezing transform in time-frequency analysis. IEEE Trans. Signal Process. 62 (1), 69–84.

[21] Wu, H.-T., 2012. Adaptive analysis of complex data sets. PhD, Princeton University.

[22] Wu, H.-T., 2013. Instantaneous frequency and wave shape functions (i). Applied and Computational Harmonic Analysis 35 (2), 181 – 199.

[23] Xiao, J., Flandrin, P., 2007. Multitaper time-frequency reassignment for nonstationary spectrum estimation and chirp enhancement. IEEE Trans. Sig. Proc. 55 (6), 2851–2860.

[24] Yang, H., 2014. Robustness analysis of synchrosqueezed transforms. arXiv:1410.5939[math.ST].

[25] Yang, H., 2015. Synchrosqueezed wave packet transforms and diffeomorphism based spectral analysis for 1D general mode decompositions. Applied and Computational Harmonic Analysis 39 (1), 33–66.

[26] Yang, H., Ying, L., 2013. Synchrosqueezed wave packet transform for 2D mode decomposition. SIAM Journal on Imaging Sciences 6 (4), 1979–2009.